

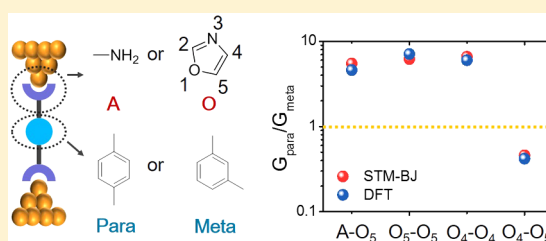
Charge Transport and Quantum Interference Effects in Oxazole-Terminated Conjugated Oligomers

Songsong Li,^{†,||,⊥} Hao Yu,^{‡,⊥} Kenneth Schwieter,[§] Kejia Chen,[‡] Bo Li,[‡] Yun Liu,^{||} Jeffrey S. Moore,^{†,§,||} and Charles M. Schroeder^{*,†,‡,§,||}

[†]Department of Materials Science and Engineering, [‡]Department of Chemical and Biomolecular Engineering, [§]Department of Chemistry, and ^{||}Beckman Institute for Advanced Science and Technology, University of Illinois at Urbana–Champaign, Urbana, Illinois 61801, United States

Supporting Information

ABSTRACT: Charge transport in single molecule junctions critically depends on the chemical identity of anchor groups used to connect molecular wires to electrodes. In this work, we report the charge transport properties of conjugated oligomers with oxazole anchors, focusing on the role of the heteroatom substitution position in terminal oxazole groups. Our results show that oxazole serves as an efficient anchor group to form stable gold–molecule–gold junctions. We further observe quantum interference (QI) effects in oxazole-terminated phenylene molecular junctions, including destructive QI in meta-substituted phenyl rings and constructive QI in para-substituted phenyl rings containing terminal oxazole groups with the same chemical constitution on both termini (i.e., O₅O₅ (5-oxazolyl) or O₄O₄ (4-oxazolyl) linkages on both termini). Surprisingly, meta-substituted phenyl rings with nonequivalent constitutions (i.e., O₄O₅ oxazole terminal linkages) show unexpectedly higher conductance as compared to para-substituted analogues. These results suggest that charge transport in oxazole-terminated molecules is determined by the heteroatom substitution position of the oxazole anchor in addition to the aryl substitution pattern of the π -conjugated core. Our results further show that conjugated molecules with homogeneous oxazole linkages obey a quantum circuit rule such that $G_{O_4-p-O_4}/G_{O_4-m-O_4} = G_{O_5-p-O_5}/G_{O_5-m-O_5}$, where G is molecular conductance. Overall, our work provides key insight into the development of new chemistries for molecular circuitry in the rapidly advancing field of single molecule electronics.



INTRODUCTION

Recent advances in single molecule electronics have uncovered new chemistries and molecular systems that offer new fundamental insight into molecular electronic structure and charge transport.^{1–6} Single molecule junctions generally contain a central bridge terminated by anchor groups that are used to connect molecular wires to electrodes.⁷ Charge transport in molecular junctions significantly depends on the chemical identity of the anchor groups and on the nature of the chemical interactions at the electrode–molecule interface.⁸ From this view, anchor groups are conveniently divided into two categories on the basis of binding interactions with metal electrodes: dative anchors bind to metal electrodes via coordination interactions, whereas covalent anchors provide direct metal–molecule contacts.⁷ Prior work has explored a wide array of anchor groups for single molecule junctions, including dative anchors with π -donor groups such as fullerene,⁹ dative anchors with lone pair donors such as primary amine ($-\text{NH}_2$),¹⁰ pyridine,^{11,12} cyano ($-\text{CN}$),¹³ isocyanate ($-\text{NC}$),¹⁴ isothiocyanate ($-\text{NCS}$),¹⁵ selenol ($-\text{Se}$),¹⁶ methyl thio ($-\text{SCH}_3$),¹⁷ phosphine,¹⁸ nitro ($-\text{NO}_2$),¹⁹ and carboxylic acid ($-\text{COOH}$),²⁰ and covalent anchors such as thiol ($-\text{SH}$),²⁰ trimethyltin,²¹ trimethylsilyl-terminated alkynes,²² and diazonium.²³

Chemical anchors are a critical component of single molecule junctions and often play a key role in determining molecular conductance in these systems. In particular, the chemical identity of dative linker groups often determines whether charge transport occurs by a highest occupied molecular orbital (HOMO)-dominated or lowest unoccupied molecular orbital (LUMO)-dominated pathway.⁷ In addition, chemical anchors have been used to tune symmetric or asymmetric coupling interactions between molecular wires and electrode surfaces. In one case, molecular design was used to install dative and covalent anchor groups at two termini of a junction, thereby generating a molecular rectifier.²⁴

Quantum interference (QI) effects play an essential role in the charge transport properties of molecular electronics.^{25,26} Single molecule conductance measurements have shown that meta-substituted phenyl groups generally exhibit lower conductance than para-substituted phenyls.²⁸ In a meta-substituted phenyl ring, the de Broglie electron waves emerge out-of-phase after traversing different molecular conduction pathways, thereby resulting in destructive QI. On the other hand, para-substituted phenyl rings give rise to constructive QI

Received: August 5, 2019

Published: September 13, 2019

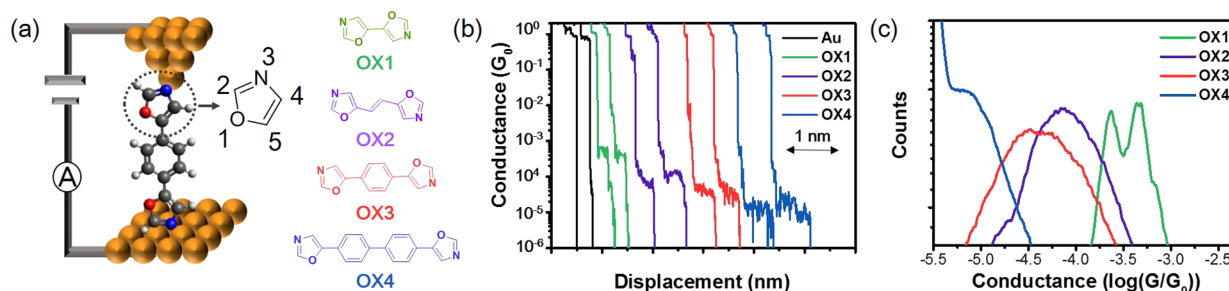


Figure 1. Charge transport in oxazole-terminated molecular wires. (a) Schematic of metal–molecule–metal junction and structures of compounds OX1–OX4. (b) Characteristic single molecule conductance traces for OX1–OX4 molecular junctions. (c) Conductance histograms for OX1–OX4, with each constructed from >10 000 traces.

Table 1. Molecular Conductance Properties of Oxazole-Terminated Phenyls, Including Average Conductance (Expressed as $\log(G/G_0)$) and $G_{\text{para}}/G_{\text{meta}}$ from STM-BJ Experiments and DFT Simulations^a

Molecule name	Structure	Log(G/G_0)	DFT Log(G/G_0)	$G_{\text{para}}/G_{\text{meta}}$	DFT $G_{\text{para}}/G_{\text{meta}}$
A-p-O ₅		-3.24	-2.78	5.5	4.6
A-m-O ₅		-3.98	-3.44		
O ₅ -p-O ₅		-4.41	-4.07	6.2	7.1
O ₅ -m-O ₅		-5.20	-4.92		
O ₄ -p-O ₄		-3.48	-3.65	6.6	6.0
O ₄ -m-O ₄		-4.30	-4.43		
O ₄ -p-O ₅		-4.77	-4.33	0.46	0.42
O ₄ -m-O ₅		-4.43	-3.95		

^aMolecule names refer to amine anchors (A), oxazole anchors linked at the 5-oxazolyl (O₅) or 4-oxazolyl (O₄) position, and arene substitution pattern (p,m).

and consequently higher levels of conductance as compared to the meta-substituted analogue.²⁵ QI effects also arise in anchor groups with conjugated rings, although only a few chemical anchors for molecule–metal junctions feature a fused ring structure. Anchor groups containing a conjugated ring structure have several potential molecular conduction pathways, complicating the molecular design of quantum circuits due to quantum effects.²⁷ Despite recent progress, the effect of heteroatom substitution position on QI effects is not fully understood in the context of anchor groups with conjugated ring structures.

In this work, we show that oxazole serves as an efficient anchor group to form stable gold–molecule–gold junctions, resulting in conductive molecular wires. We systematically explore the role of heteroatom substitution position on QI in oxazole-terminated molecular junctions using the scanning tunneling microscope break-junction (STM-BJ) technique and density functional theory (DFT) simulations. Our results show that oligophenyls terminated with oxazole exhibit an exponential conductance decay constant ($\beta = 0.40 \text{ \AA}^{-1}$), comparable to that of amine-terminated analogues ($\beta = 0.42 \text{ \AA}^{-1}$). Combined results from single molecule experiments and

molecular modeling show that the nitrogen atom in the oxazole ring is the point-of-contact to the metal surface through the lone electron pair, similar to pyridine-based anchor groups.¹¹ Our results further reveal unexpected QI phenomena in oxazole-terminated molecular junctions. For oxazole-terminated molecules with the same chemical constitution on both termini, including O₅O₅ (5-oxazolyl) or O₄O₄ (4-oxazolyl) linkages, destructive QI is observed in meta-substituted phenyl molecular junctions. Surprisingly, our results show that meta-substituted phenyl rings with non-equivalent constitutions (O₄O₅ oxazole linkages) exhibit constructive QI. Taken together, these results suggest that the heteroatom position in oxazole rings plays a key role in conductance, in addition to the arene substitution pattern in conjugated phenyl bridges. This work expands the library of chemical anchor groups and explores the effect of anchors with conjugated ring structures on QI, thereby opening new opportunities for molecular electronics.²⁹

RESULTS AND DISCUSSION

A series of oxazole-containing molecules was synthesized by van Leusen oxazole synthesis³⁰ and characterized by ¹H and

^{13}C NMR spectroscopies and mass spectrometry (Figures S1–S21). We began by synthesizing oxazole-terminated oligomers with homogeneous linkages at both termini with respect to heteroatom position on the oxazole ring. In particular, we synthesized 5,5'-bioxazole (OX1), (*E*)-1,2-bis(oxazol-5-yl)-ethene (OX2), 1,4-bis(oxazol-5-yl)benzene (OX3), and 4,4'-bis(oxazol-5-yl)-1,1'-biphenyl (OX4), all of which contain homogeneous linkages to oxazole anchors at the 5-position on the oxazole ring (Figure 1a). We further synthesized an expanded library of oxazole-terminated phenyl compounds with varying arene substitution patterns (meta- or para-linked) and defined linkages to the conjugated ring oxazole anchors (Table 1). Additional details on the synthesis and chemical characterization for all compounds can be found in Figures S1–S21.

Single molecule conductance measurements were performed using a custom-built scanning tunneling microscope break-junction (STM-BJ) technique under constant applied bias (250 mV) in a liquid solvent (1,2,4-trichlorobenzene) (Figure 1a), as previously described.^{31–33} In brief, the STM-BJ experiment is performed by measuring molecular conductance at a constant applied bias while pulling a gold tip away from a gold electrode surface, eventually leading to a break in the molecular junction. Figure 1b shows characteristic single molecule conductance traces of OX1–OX4, together with a break junction measurement in the absence of organic molecules (denoted as Au). Plateaus in molecular conductance G at values less than the quantum unit of conductance ($G_0 = 2e^2/h = 77.5 \mu\text{S}$) correspond to charge transport through organic molecules bridging the junction between the gold electrodes. Single molecule pulling experiments are generally repeated for thousands of trials to enable robust statistical analysis. In this way, one-dimensional (1D) conductance histograms are generated over a large ensemble of approximately 10^4 molecules for OX1–OX4 (Figure 1c). Interestingly, we observe two peaks in the conductance histograms for OX1 but only a single peak for OX2, OX3, and OX4. We conjecture that the two distinct conductance states in OX1 are due to two binding geometries.¹² On the other hand, OX2, OX3, and OX4 adopt a single favored binding geometry, thereby resulting in distinct conductance peaks in the 1D histograms.

Two-dimensional (2D) conductance histograms of OX1–OX4 are shown in Figure 2. 2D histograms show that average displacements during molecular pulling experiments tend to increase with increasing molecular length, such that OX4 junctions can be stretched to approximately 0.8 nm. At an applied bias of 0.25 V, we found that the signal of OX4 merged with the amplifier background noise. Therefore, we repeated the experiments and collected 2D conductance histograms of OX4 at high bias (1 V) and observed a clear separation between signal and background (Figure S22). Average molecular conductance values for OX1, OX3, and OX4 were determined from the peak values in the corresponding 1D histogram data and plotted on a semilog scale versus the distance between nitrogen atoms in terminal anchor groups for each respective molecule (Figure 3a). In all cases, the N–N distance was determined by density functional theory (DFT) and corresponds to the distance between nitrogen atoms in terminal amines for amine-terminated oligophenyls or N–N heteroatom distance between terminal oxazole rings. Our results show that the average molecular conductance follows an exponential decay as a function of molecular length, which

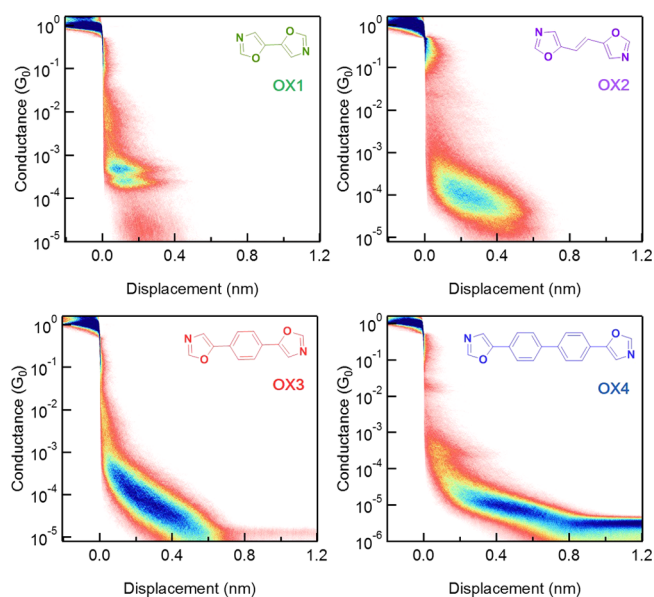


Figure 2. Two-dimensional (2D) conductance histograms for OX1–OX4, determined over a large ensemble of >10 000 individual molecules.

suggests that charge transport follows a quantum tunneling model such that $\ln(G/G_0) = -\beta L$, where β is the molecular decay constant and L is the molecular length between terminal nitrogen atoms. Using this approach, we determine a molecular decay constant $\beta = 0.40 \pm 0.01 \text{ \AA}^{-1}$ for oxazole-terminated oligophenyls, which is consistent with amine-terminated ($\beta = 0.42 \pm 0.01 \text{ \AA}^{-1}$) (Figure S23) and pyridine-terminated oligophenyls ($\beta = 0.5 \text{ \AA}^{-1}$).^{11,31} These results suggest that oxazole anchors form robust molecular contacts with metallic gold electrodes and enable stable measurements of conductance. To identify the specific anchoring site linking oxazole rings to gold electrodes, we synthesized a control molecule 1,4-di(furan-2-yl)benzene (FU1) for single molecule conductance experiments (Figure S24). In contrast to oxazole-terminated OX3, no conductance signal was observed for furan-terminated compound FU1, which confirms that the nitrogen heteroatom serves as the anchoring site in oxazole rings.

To further understand the charge transport properties of oxazole-terminated molecules, we performed molecular modeling using nonequilibrium Green's function-density functional theory (NEGF-DFT) via the Atomistix Toolkit package.³⁴ Molecular geometries for OX1–OX4 are optimized using DFT calculations performed on Spartan'16 Parallel Suite using the B3LYP functional with a 6-31G (d,p) basis set. Following the determination of geometry-optimized structures, transmission functions are determined for relaxed molecules for OX1–OX4 using NEGF-DFT (Figure 3b). For oxazole-terminated molecules OX1–OX4, the peaks in the transmission function appear between +0.1 and +0.5 eV, which corresponds to charge transport through the LUMO. We found that the slope of the transmission spectrum is positive at the Fermi level, which suggests that the conduction orbital is in an unoccupied state, the thermopower becomes negative, and electrons are transported through the LUMO in OX1–OX4.³⁵ We also found that the magnitudes of the transmission values for OX1–OX4 close to Fermi energy are consistent with conductance trends in the experimental results (Figure 3c).

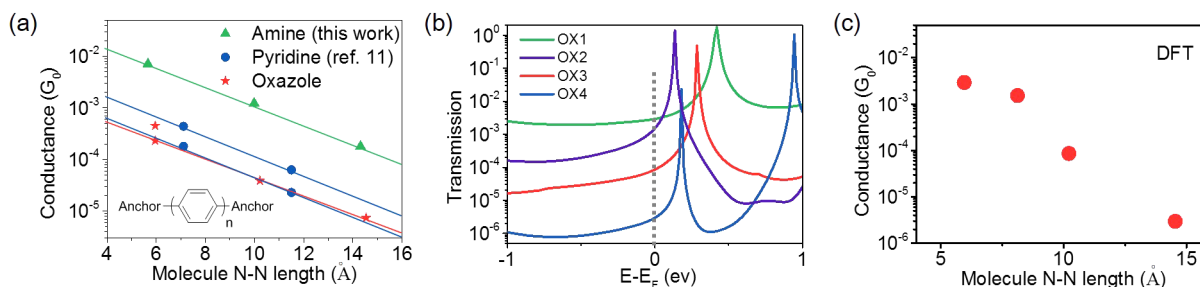


Figure 3. Charge transport behavior of oxazole-terminated oligomers determined by single molecule experiments and density functional theory (DFT) simulations. (a) Conductance peak values for amine-terminated (green, $n = 1, 2, 3$), pyridine-terminated (blue, $n = 0, 1$), and oxazole-terminated oligophenyls (red, $n = 0, 1, 2$) plotted on a semilog scale as a function of distance between N–N atoms on terminal anchors. Lines show fits to experimental data following a quantum tunneling model $G = G_0 e^{-\beta L}$. (b) Transmission spectra of OX1–OX4 determined by DFT simulations. (c) Calculated conductance values for OX1–OX4 determined from DFT simulations.

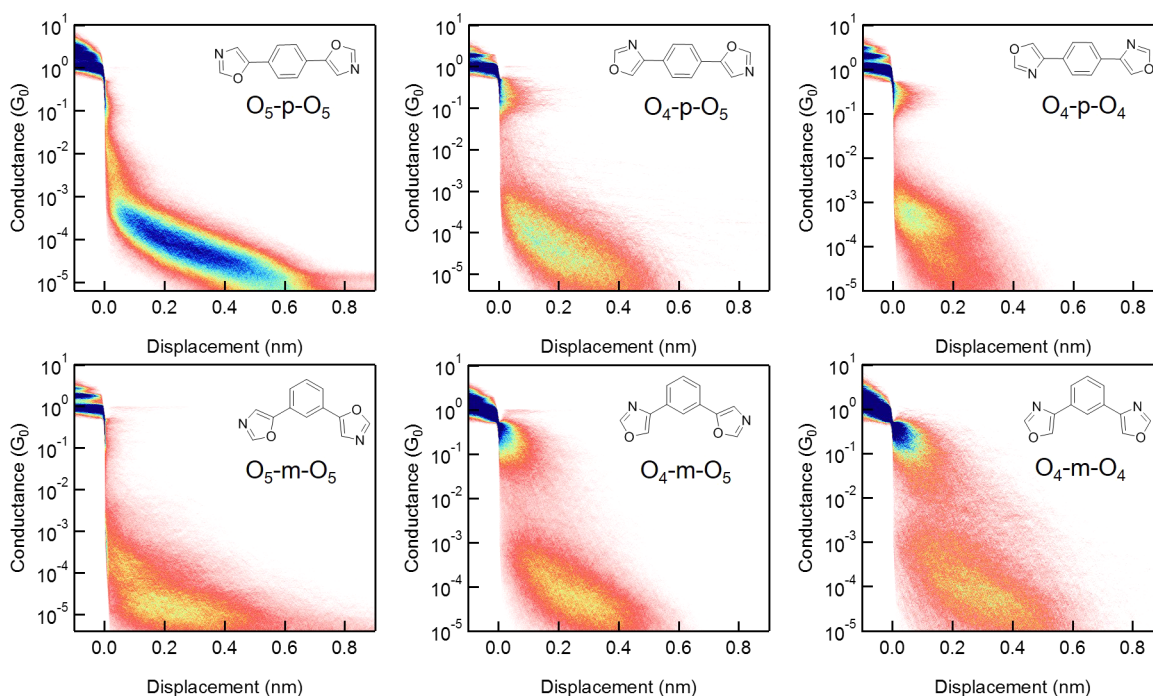


Figure 4. Two-dimensional (2D) molecular conductance histograms for a series of oxazole-terminated phenyl compounds at 0.25 V bias, each constructed from over 10 000 traces.

We next characterized the charge transport properties of a series of oxazole-terminated phenylene compounds with varying arene substitution patterns (para, meta) and different linkages to terminal oxazole groups (5-oxazolyl or 4-oxazolyl, denoted as O_5 and O_4 , respectively) (Figure 4, Figures S25–S28, and Table 1). To begin, we synthesized and studied the single molecule conductance of 1,4-bis(4-oxazolyl)benzene (O_4 -p- O_4), 1,3-bis(4-oxazolyl)benzene (O_4 -m- O_4), 1,4-bis(5-oxazolyl)benzene (O_5 -p- O_5 , also denoted as OX3), and 1,3-bis(5-oxazolyl)benzene (O_5 -m- O_5). Our results show that meta-substituted oxazole-terminated phenylenes with homogeneous O_5O_5 and O_4O_4 linkages show lower conductance than para-substituted analogues with homogeneous O_5O_5 and O_4O_4 linkages, consistent with a destructive quantum interference (QI) effect analogously observed in amine-linked,³⁶ methyl sulfide-linked,²⁷ and thiophene-linked²⁸ molecular junctions. Experimental results and NEGF-DFT simulation data in Table 1 clearly show that the QI ratio of meta/para-linkage satisfies a quantum circuit rule such that $G_{O_4\text{-p-}O_4}/G_{O_4\text{-m-}O_4} = G_{O_5\text{-p-}O_5}/G_{O_5\text{-m-}O_5} \approx 6$.^{37,38} As a comparison, pyridine-terminated

molecules also follow a quantum circuit rule such that $G_{\text{ppp}}/G_{\text{mpm}} = G_{\text{mpm}}/G_{\text{mmm}}$, where the contribution to the conductance from the central phenylene ring is independent of the anchor groups with para- or meta-linkages.²⁶ From this view, oxazole anchors offer an interesting opportunity to probe QI effects due to the asymmetric nature of the five-membered ring associated with terminal oxazole groups. For oxazole-terminated junctions with equivalent constitutions on both termini, we found that the conductance of molecules with O_4O_4 linkages is higher as compared to their counterparts with O_5O_5 linkages based on most-probable conductance results and NEGF-DFT simulations, which further supports the quantum circuit rule $G_{O_4\text{-p-}O_4}/G_{O_5\text{-p-}O_5} = G_{O_4\text{-m-}O_4}/G_{O_5\text{-m-}O_5}$.

To further examine QI effects through oxazole-terminated molecular junctions with nonequivalent constitutions on both termini, we synthesized and studied the molecular conductance of 5-(4-(oxazol-4-yl)phenyl)oxazole (O_4 -p- O_5) and 5-(3-(oxazol-4-yl)phenyl)oxazole (O_4 -m- O_5). From the most-probable conductance results and NEGF-DFT simulations, our results show that the conductance of O_4 -p- O_5 is lower than

that of $O_4\text{-m-O}_5$, such that $G_{O_4\text{-p-O}_5}/G_{O_4\text{-m-O}_5} < 0.5$. Surprisingly, these results suggest that the meta-substituted phenylene exhibits a higher conductance than the para-substituted phenylene in oxazole-terminated molecules with heterogeneous O_4O_5 linkages. Recently, Li et al.³⁹ and Huang et al.⁴⁰ used electrochemical gating to tune QI, which revealed that meta-substituted phenyl groups show higher conductance than para-substituted phenyls. On the other hand, our results show that a meta-substituted phenylene group can exhibit a higher molecular conductance relative to the para-substituted analogue without external electrochemical gating.⁴¹ In prior work, Borges et al. reported that meta-coupled bipyridine molecules show higher conductance through a σ -bonded system as compared to the para-coupled analogue.⁴² For $O_4\text{-m-O}_5$, the electronic coupling occurs across seven bonds, whereas for $O_4\text{-p-O}_5$ the coupling is through eight bonds. Therefore, we posit that $O_4\text{-m-O}_5$ has a higher σ contribution to charge transport, which gives rise to a larger total transmission for $O_4\text{-m-O}_5$ as compared to $O_4\text{-p-O}_5$. Similar observations were reported by Gorczak and co-workers,⁴³ who showed that meta-substituted biphenyl bridges exhibit a higher hole transfer rate as compared to para-substituted analogues. Interestingly, this phenomenon was attributed to the asymmetric donor and acceptor states, which lead to asymmetry in the molecular orbitals. In our work, we studied the molecular conductance of phenylenes containing heterogeneous anchor groups based on oxazole-terminated O_4O_5 linkages. For such heterogeneous linked molecules, we conjecture that one anchor group contributes constructive QI and the second anchor results in destructive QI. When coupled with a meta-substituted phenylene bridge with destructive QI, heterogeneous oxazole O_4O_5 linkages can alter the overall QI in the molecular junction, thereby giving rise to unexpectedly high conductance in the meta-linked molecular bridge.

CONCLUSION

In this work, we study the charge transport properties of a series of oxazole-terminated phenylene compounds with varying arene substitution patterns (para, meta) and different linkages to terminal oxazole rings using a combination of single molecule experiments and molecular models. Our results show that oxazole serves as a stable chemical anchor group for facilitating molecular connections to gold metal electrode surfaces. Oxazole-terminated (O_5 linkage) oligophenylys exhibit a decay constant $\beta = 0.40 \pm 0.01 \text{ \AA}^{-1}$, which is comparable to amine-terminated and pyridine-terminated equivalents. In addition, we systematically studied QI phenomena through the central phenyl ring and terminal oxazole ring. In particular, for oxazole-terminated junctions with equivalent constitutions on both termini, which include O_4O_4 and O_5O_5 oxazole-terminated molecules, the QI of the central phenylene follows a quantum circuit rule that $G_{O_4\text{-p-O}_4}/G_{O_4\text{-m-O}_4} = G_{O_5\text{-p-O}_5}/G_{O_5\text{-m-O}_5}$. For oxazole-terminated junctions with nonequivalent constitutions on both termini, including O_4O_5 oxazole-terminated molecules, meta-substituted phenylene exhibits a higher conductance as compared to para-substituted phenylene. These results reveal the role of the anchor group in controlling QI, which facilitates an increased understanding of molecular conductance in junctions with complex heterogeneous structures. Moving forward, this work could aid in the design and development of new chemistries for molecular electronics.

ASSOCIATED CONTENT

Supporting Information

The Supporting Information is available free of charge on the ACS Publications website at DOI: 10.1021/jacs.9b08427.

Description of chemical synthesis, chemical and physical characterization of oxazole-terminated molecules, experimental details on STM-BJ, simulation methods, supporting text, and supporting figures (PDF)

AUTHOR INFORMATION

Corresponding Author

*cms@illinois.edu

ORCID

Yun Liu: 0000-0001-7077-363X

Charles M. Schroeder: 0000-0001-6023-2274

Author Contributions

[†]S.L. and H.Y. contributed equally to this work.

Notes

The authors declare no competing financial interest.

ACKNOWLEDGMENTS

We thank Prof. Latha Venkataraman and Dr. Yaping Zang for generously providing advice in building the STM-BJ instrument. This work was supported by the U.S. Department of Defense by a MURI (Multi-University Research Initiative) through the Army Research Office (ARO) through award W911NF-16-1-0372 to C.M.S. and J.S.M.

REFERENCES

- (1) Aviram, A.; Ratner, M. A. Molecular rectifiers. *Chem. Phys. Lett.* **1974**, *29*, 277.
- (2) Xu, B.; Tao, N. J. Measurement of single-molecule resistance by repeated formation of molecular junctions. *Science* **2003**, *301*, 1221.
- (3) Metzger, R. M. Unimolecular electronics. *Chem. Rev.* **2015**, *115*, 5056.
- (4) Aradhya, S. V.; Venkataraman, L. Single-molecule junctions beyond electronic transport. *Nat. Nanotechnol.* **2013**, *8*, 399.
- (5) Xin, N.; Guan, J.; Zhou, C.; Chen, X.; Gu, C.; Li, Y.; Ratner, M. A.; Nitzan, A.; Stoddart, J. F.; Guo, X. Concepts in the design and engineering of single-molecule electronic devices. *Nature Reviews Physics* **2019**, *1*, 211.
- (6) Zang, Y.; Pinkard, A.; Liu, Z.-F.; Neaton, J. B.; Steigerwald, M. L.; Roy, X.; Venkataraman, L. Electronically Transparent Au -N Bonds for Molecular Junctions. *J. Am. Chem. Soc.* **2017**, *139*, 14845.
- (7) Su, T. A.; Neupane, M.; Steigerwald, M. L.; Venkataraman, L.; Nuckolls, C. Chemical principles of single-molecule electronics. *Nature Reviews Materials* **2016**, *1*, 16002.
- (8) Leary, E.; La Rosa, A.; Gonzalez, M. T.; Rubio-Bollinger, G.; Agrait, N.; Martin, N. Incorporating single molecules into electrical circuits. The role of the chemical anchoring group. *Chem. Soc. Rev.* **2015**, *44*, 920.
- (9) Martin, C. A.; Ding, D.; Sørensen, J. K.; Bjørnholm, T.; van Ruitenbeek, J. M.; van der Zant, H. S. Fullerene-based anchoring groups for molecular electronics. *J. Am. Chem. Soc.* **2008**, *130*, 13198.
- (10) Venkataraman, L.; Klare, J. E.; Tam, I. W.; Nuckolls, C.; Hybertsen, M. S.; Steigerwald, M. L. Single-molecule circuits with well-defined molecular conductance. *Nano Lett.* **2006**, *6*, 458.
- (11) Kamenetska, M.; Quek, S. Y.; Whalley, A.; Steigerwald, M.; Choi, H.; Louie, S. G.; Nuckolls, C.; Hybertsen, M.; Neaton, J.; Venkataraman, L. Conductance and geometry of pyridine-linked single-molecule junctions. *J. Am. Chem. Soc.* **2010**, *132*, 6817.
- (12) Kim, T.; Darancet, P.; Widawsky, J. R.; Kotiuga, M.; Quek, S. Y.; Neaton, J. B.; Venkataraman, L. Determination of Energy Level

Alignment and Coupling Strength in 4,4'-Bipyridine Single-Molecule Junctions. *Nano Lett.* **2014**, *14*, 794.

(13) Mishchenko, A.; Zotti, L. A.; Vonlanthen, D.; Bürkle, M.; Pauly, F.; Cuevas, J. C.; Mayor, M.; Wandlowski, T. Single-Molecule Junctions Based on Nitrile-Terminated Biphenyls: A Promising New Anchoring Group. *J. Am. Chem. Soc.* **2011**, *133*, 184.

(14) Kim Beebe, J. M.; Jun, Y.; Zhu, X. Y.; Frisbie, C. D. Correlation between HOMO Alignment and Contact Resistance in Molecular Junctions: Aromatic Thiols versus Aromatic Isocyanides. *J. Am. Chem. Soc.* **2006**, *128*, 4970.

(15) Ko, C.-H.; Huang, M.-J.; Fu, M.-D.; Chen, C.-h. Superior Contact for Single-Molecule Conductance: Electronic Coupling of Thiolate and Isothiocyanate on Pt, Pd, and Au. *J. Am. Chem. Soc.* **2010**, *132*, 756.

(16) Yasuda, S.; Yoshida, S.; Sasaki, J.; Okutsu, Y.; Nakamura, T.; Taninaka, A.; Takeuchi, O.; Shigekawa, H. Bond fluctuation of S/Se anchoring observed in single-molecule conductance measurements using the point contact method with scanning tunneling microscopy. *J. Am. Chem. Soc.* **2006**, *128*, 7746.

(17) Garner, M. H.; Li, H.; Chen, Y.; Su, T. A.; Shangguan, Z.; Paley, D. W.; Liu, T.; Ng, F.; Li, H.; Xiao, S.; Nuckolls, C.; Venkataraman, L.; Solomon, G. C. Comprehensive suppression of single-molecule conductance using destructive σ -interference. *Nature* **2018**, *558*, 415.

(18) Kamenetska, M.; Koentopp, M.; Whalley, A.; Park, Y.; Steigerwald, M.; Nuckolls, C.; Hybertsen, M.; Venkataraman, L. Formation and evolution of single-molecule junctions. *Phys. Rev. Lett.* **2009**, *102*, 126803.

(19) Zotti, L. A.; Kirchner, T.; Cuevas, J. C.; Pauly, F.; Huhn, T.; Scheer, E.; Erbe, A. Revealing the role of anchoring groups in the electrical conduction through single-molecule junctions. *Small* **2010**, *6*, 1529.

(20) Chen, F.; Li, X.; Hihath, J.; Huang, Z.; Tao, N. Effect of anchoring groups on single-molecule conductance: comparative study of thiol-, amine-, and carboxylic-acid-terminated molecules. *J. Am. Chem. Soc.* **2006**, *128*, 15874.

(21) Batra, A.; Kladnik, G.; Gorjizadeh, N.; Meisner, J.; Steigerwald, M.; Nuckolls, C.; Quek, S. Y.; Cvetko, D.; Morgante, A.; Venkataraman, L. Trimethyltin-mediated covalent gold-carbon bond formation. *J. Am. Chem. Soc.* **2014**, *136*, 12556.

(22) Hong, W.; Li, H.; Liu, S.-X.; Fu, Y.; Li, J.; Kaliginedi, V.; Decurtins, S.; Wandlowski, T. Trimethylsilyl-terminated oligo (phenylene ethynylene) s: an approach to single-molecule junctions with covalent Au-C σ -bonds. *J. Am. Chem. Soc.* **2012**, *134*, 19425.

(23) Hines, T.; Diez-Pérez, I.; Nakamura, H.; Shimazaki, T.; Asai, Y.; Tao, N. Controlling Formation of Single-Molecule Junctions by Electrochemical Reduction of Diazonium Terminal Groups. *J. Am. Chem. Soc.* **2013**, *135*, 3319.

(24) Batra, A.; Darancet, P.; Chen, Q. S.; Meisner, J. S.; Widawsky, J. R.; Neaton, J. B.; Nuckolls, C.; Venkataraman, L. Tuning Rectification in Single-Molecular Diodes. *Nano Lett.* **2013**, *13*, 6233.

(25) Lambert, C. Basic concepts of quantum interference and electron transport in single-molecule electronics. *Chem. Soc. Rev.* **2015**, *44*, 875.

(26) Manrique, D. Z.; Huang, C.; Baghernejad, M.; Zhao, X.; Al-Owaedi, O. A.; Sadeghi, H.; Kaliginedi, V.; Hong, W.; Gulcur, M.; Wandlowski, T. A quantum circuit rule for interference effects in single-molecule electrical junctions. *Nat. Commun.* **2015**, *6*, 6389.

(27) Aradhya, S. V.; Meisner, J. S.; Krikorian, M.; Ahn, S.; Parameswaran, R.; Steigerwald, M. L.; Nuckolls, C.; Venkataraman, L. Dissecting contact mechanics from quantum interference in single-molecule junctions of stilbene derivatives. *Nano Lett.* **2012**, *12*, 1643.

(28) Arroyo, C. R.; Tarkuc, S.; Frisenda, R.; Seldenthuis, J. S.; Woerde, C. H.; Eelkema, R.; Grozema, F. C.; van der Zant, H. S. Signatures of quantum interference effects on charge transport through a single benzene ring. *Angew. Chem.* **2013**, *125*, 3234.

(29) Xiang, D.; Wang, X.; Jia, C.; Lee, T.; Guo, X. Molecular-Scale Electronics: From Concept to Function. *Chem. Rev.* **2016**, *116*, 4318.

(30) Van Leusen, A.; Hoogenboom, B.; Siderius, H. A novel and efficient synthesis of oxazoles from tosylmethylisocyanide and carbonyl compounds. *Tetrahedron Lett.* **1972**, *13*, 2369.

(31) Venkataraman, L.; Klare, J. E.; Nuckolls, C.; Hybertsen, M. S.; Steigerwald, M. L. Dependence of single-molecule junction conductance on molecular conformation. *Nature* **2006**, *442*, 904.

(32) Zang, Y.; Ray, S.; Fung, E.-D.; Borges, A.; Garner, M. H.; Steigerwald, M. L.; Solomon, G. C.; Patil, S.; Venkataraman, L. Resonant Transport in Single-Diketopyrrolopyrrole Junctions. *J. Am. Chem. Soc.* **2018**, *140*, 13167.

(33) Li, B.; Yu, H.; Montoto, E.; Liu, Y.; Li, S.; Schwieter, K.; Rodríguez-López, J.; Moore, J. S.; Schroeder, C. M. Intrachain Charge Transport through Conjugated Donor-Acceptor Oligomers. *ACS Applied Electronic Materials* **2019**, *1*, 7.

(34) Cai, Z.; Lo, W.-Y.; Zheng, T.; Li, L.; Zhang, N.; Hu, Y.; Yu, L. Exceptional single-molecule transport properties of ladder-type heteroacene molecular wires. *J. Am. Chem. Soc.* **2016**, *138*, 10630.

(35) Komoto, Y.; Fujii, S.; Iwane, M.; Kiguchi, M. Single-molecule junctions for molecular electronics. *J. Mater. Chem. C* **2016**, *4*, 8842.

(36) Kiguchi, M.; Nakamura, H.; Takahashi, Y.; Takahashi, T.; Ohto, T. Effect of anchoring group position on formation and conductance of a single disubstituted benzene molecule bridging Au electrodes: change of conductive molecular orbital and electron pathway. *J. Phys. Chem. C* **2010**, *114*, 22254.

(37) Lambert, C. J.; Liu, S. X. A Magic Ratio Rule for Beginners: A Chemist's Guide to Quantum Interference in Molecules. *Chem. - Eur. J.* **2018**, *24*, 4193.

(38) Sangtarash, S.; Huang, C.; Sadeghi, H.; Sorohhov, G.; Hauser, J. R.; Wandlowski, T.; Hong, W.; Decurtins, S.; Liu, S.-X.; Lambert, C. J. Searching the hearts of graphene-like molecules for simplicity, sensitivity, and logic. *J. Am. Chem. Soc.* **2015**, *137*, 11425.

(39) Li, Y.; Buerkle, M.; Li, G.; Rostamian, A.; Wang, H.; Wang, Z.; Bowler, D. R.; Miyazaki, T.; Xiang, L.; Asai, Y.; Zhou, G.; Tao, N. Gate controlling of quantum interference and direct observation of anti-resonances in single molecule charge transport. *Nat. Mater.* **2019**, *18*, 357.

(40) Huang, B.; Liu, X.; Yuan, Y.; Hong, Z.-W.; Zheng, J.-F.; Pei, L.-Q.; Shao, Y.; Li, J.-F.; Zhou, X.-S.; Chen, J.-Z. Controlling and Observing Sharp-Valleyed Quantum Interference Effect in Single Molecular Junctions. *J. Am. Chem. Soc.* **2018**, *140*, 17685.

(41) Li, X.; Tan, Z.; Huang, X.; Bai, J.; Liu, J.; Hong, W. Experimental investigation of quantum interference in charge transport through molecular architectures. *J. Mater. Chem. C* **2019**, *1* DOI: 10.1039/C9TC02626F.

(42) Borges, A.; Fung, E. D.; Ng, F.; Venkataraman, L.; Solomon, G. C. Probing the Conductance of the σ -System of Bipyridine Using Destructive Interference. *J. Phys. Chem. Lett.* **2016**, *7*, 4825.

(43) Gorczak, N.; Renaud, N.; Tarkuc, S.; Houtepen, A. J.; Eelkema, R.; Siebbeles, L. D.; Grozema, F. C. Charge transfer versus molecular conductance: molecular orbital symmetry turns quantum interference rules upside down. *Chemical Science* **2015**, *6*, 4196.